HNK-1 in Morphological Study of Development of the Cardiac Conduction System in Selected Groups of Sauropsida

ALENA KVASILOVA [1], MARTINA GREGOROVICOVA [1,2], MARTIN KUNDRAT [3] AND DAVID SEDMERA [1,2*]

[1]Institute of Anatomy, Charles University, Prague, Czech Republic
[2]Institute of Physiology, The Czech Academy of Sciences, Prague, Czech Republic
[3]Center for Interdisciplinary Biosciences, Innovation and Technology Park, University of Pavol Jozef Safarik, Kosice, Slovak Republic

ABSTRACT

Human natural killer (HNK)-1 antibody is an established marker of developing cardiac conduction system (CCS) in birds and mammals. In our search for the evolutionary origin of the CCS, we tested this antibody in a variety of sauropsid species (*Crocodylus niloticus, Varanus indicus*, *Pogona vitticeps*, *Pantherophis guttatus, Eublepharis macularius, Gallus gallus,* and *Coturnix japonica*). Hearts of different species were collected at various stages of embryonic development and studied to map immunoreactivity in cardiac tissues. We performed detection on alternating serial paraffin sections using immunohistochemistry for smooth muscle actin or sarcomeric actin as myocardial markers, and HNK-1 to visualize overall staining pattern and then positivity in specific myocyte populations. We observed HNK-1 expression of various intensity distributed in the extracellular matrix and mesenchymal cell surface of cardiac cushions in most of the examined hearts. Strong staining was found in the cardiac nerve fibers and ganglia in all species. The myocardium of the sinus venosus and the atrioventricular canal exhibited transitory patterns of expression. In the *Pogona* and *Crocodylus* hearts, as well as in the *Gallus* and *Coturnix* ones, additional expression was detected in a subset of myocytes of the (inter) ventricular septum. These results support the use of HNK-1 as a conserved marker of the CCS and suggest that there is a rudimentary CCS present in developing reptilian hearts. Anat Rec, 2018. © 2018 Wiley Periodicals, Inc.

Key words: Leu 7; CD 57; immunohistochemistry; heart; reptile

The HNK-1 monoclonal antibody is a marker for early migrating neural crest cells (NCC), but reacts also with structures, which are not derived from the neural crest (Gorza et al., 1988; Luider et al., 1993). Human natural killer (HNK)-1, (the CD57 antigen or LEU7) is expressed as a carbohydrate epitope that contains a sulfoglucuronyl residue in several adhesion molecules of the nervous system (Nakajima et al., 2001). HNK-1 epitope is also

Grant sponsor: Grant Agency of the Academy of Sciences of the Czech Republic; Grant number: KJB6111301; Grant sponsor: Grantová Agentura České Republiky; Grant number: 16-02972S and 13-12412S; Grant sponsor: Ministry of Education, Youth and Sports of the Czech Republic; Grant number: PROGRES-Q38 and COST LTC17023, MEYS (LM2015062 Cze; Grant sponsor: NATO Fellowship Programme; Grant number: 13/2003-Czech Republic; Grant sponsor: Czech Academy of Sciences; Grant sponsor: Ministry of Education, Youth and Sports; Grant sponsor: Grant Agency of the Czech Republic.

*Correspondence to: David Sedmera, Charles University in Prague, First Faculty of Medicine, Institute of Anatomy, U Nemocnice 3, 12800 Prague 2, Czech Republic. E-mail: david.sedmera@lf1.cuni.cz

Received 11 January 2018; Revised 31 May 2018; Accepted 11 June 2018.

DOI: 10.1002/ar.23925
Published online in Wiley Online Library (wileyonlinelibrary.com).

expressed in a subset of myocytes in the developing cardiac conduction system (CCS), making it a very useful, conserved marker for visualizing the CCS in mammals and birds (Nakagawa et al., 1993; Chuck and Watanabe, 1997). Apart from a constant pattern of HNK-1 antigen expression during development, stage-dependent HNK-1 antigen expression was also found (Aoyama et al., 1993; DeRuiter et al., 1995).

HNK-1 epitope was described in the neural cells in *Danio* (Wilson et al., 1990) and *Xenopus* (Nordlander, 1989), suggesting that the conservation of this glycan, or rather group of enzymes involved in its synthesis, is conserved in vertebrates.

Ventricular septation in Sauropsida varies among species, which means that we can find a range from fully septated heart in archosaurs (crocodylians and birds) (Webb, 1979), almost septated heart in varanids and pythons (Webb et al., 1971; Jensen et al., 2010) to feebly developed septum in nonvaranid lizards and snakes with the exception of Pythonidae (Jensen et al., 2013a, 2014). The nomenclature of the heart structures in squamates is not unified. For clarity's sake, we follow here the nomenclature as could be found in Jensen et al. (2014). In squamates, there are three septa in the ventricle—muscular ridge, bulbuslamelle, and ventricular septum (Jensen et al., 2014). These structures are developed according to life-histories of the squamate—it means that they reflect lifestyles of the species more than their position on the phylogenetic tree (Burggren, 1988). There is a clear link among lifestyle and ventricular septation in particular species: it seems that the level of septation of the ventricle could be a derived state, highly reduced or developed in squamates (Moorman and Christoffels, 2003).

The reptiles are the first group of tetrapods fully independent from the aquatic environment. Physiologically, they have a variable body temperature and correspondingly slower metabolism and heart rate. Unlike the fishes and amphibians, however, which do have common model species as representatives (zebrafish and xenopus or axolotl, respectively), they are seldom studied in the laboratory settings. Consequently, little is known about their heart and even less about its electrophysiology. Morphologically, their hearts range from highly trabeculated ones very similar to those of amphibians to fully septated (but still heavily trabeculated) hearts of crocodiles, similar to those of the homeiotherms (birds and mammals).

Sauropsida as a sister group to Synapsida (Laurin and Reisz, 1995) number thousands of species including on the one hand Aves and Crocodylia, known together as Archosauria (Benton and Clark, 1988; Nesbitt et al., 2013), and on the other hand Chelonia as a sister group to Archosauria (Chiari et al., 2012), and Lepidosauria, which cover two clades—Sphenodontia (Rest et al., 2003; Cree, 2014) and Squamata (Pyron et al., 2013). Although in Squamate reptiles the conduction tissues were recently studied to some extent (Jensen et al., 2014), its embryonic development is not clear and only a few comparative studies exist (Jensen et al., 2012, 2013a, 2013b; Gregorovicova et al., 2018). In Tetrapods the complete septation of the heart evolved in three lineages independently (Jensen et al., 2013b)—these well-known lineages are mammals, birds, and crocodylians. In case of mammals and birds there exists a premise that the reason why they both have completely septated heart is endothermy and associated high heart rate (Davies, 1942). However, situation is complicated in crocodylians, which also have fully septated heart (Webb, 1979; Koshiba-Takeuchi et al., 2009; Poelmann et al., 2017) while all the extant taxa are purely ectothermic (Grigg and Kirshner, 2015). This messy situation continues within the squamate reptiles, which present a large variation in the extent of ventricular septation feebly hearts (typical lizards) to almost fully septated ones in varanids (White, 1968; Webb et al., 1971, 1974; Burggren, 1988). Since it seems that this more extensively septated state in squamates is a derived one (Moorman and Christoffels, 2003) and that the reptilian heart is generally highly specialized for shunting (Hicks and Wang, 1996), we focused our attention on Sauropsida to compare the state of development of the CCS in archosaurs (*Crocodylus niloticus* and *Gallus gallus*) with the squamates. Crocodylians show clear positivity for the CCS marker HNK-1 within the embryonic heart (Kundrat, 2008) similar to the chick (Chuck and Watanabe, 1997), which was chosen as a "positive control." In case of squamates, we chose representative species across squamate taxa with focusing on their lifestyle (Adolph and Porter, 1993; Shine, 2005) as well as on their position in the phylogenetic tree (Pyron et al., 2013). These species are Leopard Gecko (*Eublepharis macularius*), which represents the basal taxa with nocturnal lifestyle (Seufer et al., 2005). Central Bearded Dragon (*Pogona vitticeps*) was selected as a representative of higher taxa with higher metabolism than Leopard Gecko due to its diurnal lifestyle (Köhler et al., 2003). As a crown species of the phylogenetic tree of squamates was chosen Mangrove Monitor (*Varanus indicus*) as an active predator (Pianka and King, 2004) with mammalian-like pressure differentials between the pulmonary and systemic circuits with its metabolic rate considerably higher than in the other squamate reptiles (Thompson and Withers, 1997; Wang et al., 2003). The last species, Corn Snake (*Pantherophis guttatus*), represents the group of extremely diverse squamate reptiles—snakes, whose position in phylogenetic tree is still unresolved (Lee, 1997; Vidal and Hedges, 2005; Pyron et al., 2013). The Corn Snake as an example of ophidian represents a unique state thanks to its morphologically distinctive form representing a departure from the typical 'Bauplan' of squamate reptiles (Wiens and Slingluff, 2001). Another factor playing an important role in selection of the particular species was the availability of fertilized eggs from captivity-bred animals.

In mammals, expression of the HNK-1 epitope in the developing heart was described in the rat (Wenink et al., 2000), human (Blom et al., 1999), rabbit (Gorza et al., 1988), dog (Wilson et al., 1990), and dromedary (El Sharaby et al., 2001). However, the antigen is not expressed in mouse (Wilson et al., 1990). While in the rat, rabbit, and human embryonic heart the expression patterns are similar both developmentally and in three-dimensional reconstruction and mark the developing CCS in addition to cardiac nerves, in dromedary, only neural expression was reported. So, while certainly useful and conserved, the specificity needs to be validated for each organism.

There are recent reports on HNK1 use to study development of neural crest and cranial nerves in the embryonic Nile crocodile (Kundrat, 2008; Kundrat, 2009). There was also a mention of expression in the developing heart, but no figure documentation was provided. We thus

undertook a comprehensive evaluation of these histological series, complemented with our own sampling of various embryonic reptilian species. Our choice, dictated in part by the availability of eggs and embryonic material, aimed to cover a range of septation states—from a very rudimentary septum in *E. macularius* through partly septated ventricle in *P. vitticeps* and *P. guttatus*, almost fully septated ventricle of varanids to completely septated (from later stages) heart of *C. niloticus.* For the reference, we used also chick embryos to study the possible effect of different fixatives on staining patterns, and a few quail (*Coturnix japonica,* Temminck and Schlegel, 1849) embryonic hearts to verify the potential of generalization of findings in the chick to other avians. We hypothesized that the extent of HNK-1 immunostaining, and thus development of conduction system, will correlate with the degree of ventricular septation. We found that while HNK-1 stained consistently neural tissues in all examined species, the patterns of expression in various cardiac populations were species- and stage-dependent. We observed expression in the extracellular matrix and mesenchymal cells of cardiac cushions, subendocardium, and also different myocardial populations (sinus venosus—the cardiac pacemaker region, atrioventricular canal, and subpopulation of ventricular myocytes). We conclude that HNK-1 could be used as a conserved marker of CCS, as it is expressed in similar myocyte populations across most amniotes.

1. MATERIALS AND METHODS

1.1 Sample Preparation

List of the examined species, stages and number of specimens is presented in Tables 1–6.

Serial sections of the *C. niloticus* embryos stained with HNK-1 and hematoxylin from previous studies (Kundrat, 2008; Kundrat, 2009) were used for the crocodile model. Hearts of *V. indicus* were isolated from embryos originating in the collection assembled previously for the staging purposes (Gregorovicova et al., 2012). Hearts from the other species were extracted from the embryos submerged in a cold buffer optimized for reptiles (Jensen et al., 2012), or Tyrode's for the avian species (*G. gallus*

TABLE 1. Number of *Crocodylus niloticus* embryonic hearts analyzed by HNK-1 immunohistochemistry at different stages

Ferguson stage	Number analyzed
St. 0	2
St. 1	1
St. 2	1
St. 2–3	2
St. 3	5
St. 4	8
St. 5	3
St. 6	2
St. 7	4
St. 8	2
St. 9	1
St. 9–10	1
St. 10	1
St. 10–11	2
St. 11	2
St. 12	1
St. 13	1
Total	**39**

This range corresponds to days 0–17 postoviposition (dpo) with noted variability among clutches (total of five different nests). The material is derived from study by Kundrat (2008).

TABLE 2. Number of *Varanus indicus* embryonic hearts analyzed at different developmental stages

Day postoviposition	Number analyzed
43 dpo	1
63 dpo	1
95 dpo	1
103 dpo	1
Total	4

Selected samples originating from a larger collection assembled by Gregorovicova et al. (2012).

TABLE 3. Number of *Pogona vitticeps* embryonic hearts analyzed at different developmental stages

Day postoviposition	Number analyzed
14 dpo	2
17 dpo	1
18 dpo	2
23 dpo	1
28 dpo	1
30 dpo	1
31 dpo	1
35 dpo	2
39 dpo	1
41 dpo	1
46 dpo	1
49 dpo	1
55 dpo	1
62 dpo	1
68 dpo	1
Total	18

TABLE 4. Number of *Pantherophis guttatus* embryonic hearts analyzed at different developmental stages

Day postoviposition	Number analyzed
9 dpo	1
16 dpo	1
23 dpo	1
32 dpo	1
Total	4

TABLE 5. Number of *Eublepharis macularius* embryonic hearts analyzed at different developmental stages

Day postoviposition	Number analyzed
7 dpo	1
11 dpo	1
15 dpo	1
18 dpo	1
26 dpo	1
32 dpo	1
40 dpo	1
47 dpo	1
53 dpo	1
Total	9

TABLE 6. Number of *Gallus gallus* embryonic hearts analyzed at different days of incubation

Embryonic day	Number analyzed
ED 4	7
ED 5	3
ED 6	7
ED 7	2
ED 8	12
ED 9	2
ED 10	8
ED 12	4
ED 13	1
ED 14	8
ED 16	5
ED 18	2
ED 20	2
Total	63

and *C. japonica*) after rapid recording of their external appearance for documentation and staging purposes, fixed overnight in 4% paraformaldehyde solution in phosphate buffered saline (PBS) on ice with gentle rocking. Sampling of embryonic tissues from the eggs is exempt from animal protection legislation in the Czech Republic; however, care was taken to minimize any potential suffering of the embryos by using ice-cold dissection buffer and rapid decapitation as the method of euthanasia. After fixation, they were rinsed thrice in PBS and then dehydrated in a series of ethanols, followed by clearing in benzene, and then embedded in paraplast. Eight to 10 μm sections were cut on a microtome, and alternating sections (four sets) were mounted on poly-lysine coated slides. Three sets of slides were processed for immunohistochemistry as described below, while the remaining series was preserved for further investigations (double immunolabeling).

1.2 Immunohistochemistry

The sections were deparaffinized and rinsed once with PBS for 5 min, permeabilized twice with PBS/0.5% Tween 20 for 5 min and rinsed once with PBS for 5 min. Afterwards the sections were blocked with 10% normal goat serum (NGS) for an hour at room temperature, and then incubated overnight at +4°C with primary antibodies. The following antibodies and dilutions were used: mouse monoclonal IgM heavy chains and kappa light chains to HNK-1 (1:100; Beckton Dickinson #347390), mouse monoclonal IgG2a isotype to Alpha Smooth Muscle Action (SMA, 1:800; Sigma #A2547), and mouse monoclonal IgM isotype to Alpha Sarcomeric Actin (SA, 1:500; Sigma #A2172).

On the next day, the sections were rinsed in three changes of PBS and Horseradish Peroxidase (HRP)-conjugated Goat Anti-Mouse secondary antibody (1:200; Jackson ImmunoResearch #115-035-068) was applied for 90 min at room temperature. Primary and secondary antibodies were diluted in PBS that contained 0.1%

TABLE 7. HNK-1 expression in different areas of *Crocodylus niloticus* embryonic hearts sampled at different developmental stages (Ferguson, 1985)

Ferguson stage	AV-cushions	AV-canal	Sinus venosus	AV-sulcus—nerves	Ventricle	Atria	Valves	Aortic trunk
St. 0	0	0	0	0	0	0	0	0
St. 1	0	0	0	0	0	0	0	0
St. 2	0	0	0	0	0	0	0	0
St. 2–3	0	0	0	0	0	0	0	0
St. 3	0	0	0	0	0	0	0	0
St. 4	0	0	0	0	0	0	0	0
St. 5	0	0	0	0	0	0	0	0
St. 6	0	1	0	0	1	1	0	0
St. 7	0	0	0	0	0	0	0	0
St. 8	0	0	1	0	0	0	0	0
St. 9	0	0	0	0	0	0	0	0
St. 9–10	0	0	1	0	0	1	0	0
St. 10	0	0	1	1	0	0	0	0
St. 10–11	0	0	0	0	0	0	0	0
St. 11	0	0	0	0	1	0	0	0
St. 12	0	0	0	0	1	0	0	0
St. 13	0	0	1	0	0	0	0	0

0, no expression observed; 1, expression detected.

TABLE 8. HNK-1 expression in different areas of *Varanus indicus* embryonic hearts sampled at different developmental stages

AGE	AV-cushions	AV-canal	Sinus venosus	AV-sulcus—nerves	Ventricle	Atria	Valves	Aortic trunk
43 dpo	1	0	1	1	0	0	1	1
63 dpo	1	1	1	1	0	0	1	1
95 dpo	0	1	1	1	1	1	1	1
103 dpo	0	1	1	1	1	1	1	1

Selected samples originating from collection assembled by Gregorovicova et al. (2012).

TABLE 9. HNK-1 expression in different areas of *Pogona vitticeps* embryonic hearts sampled at different developmental stages

AGE	AV-cushions	AV-canal	Sinus venosus	AV-sulcus—nerves	Ventricle	Atria	Valves	Aortic trunk
14 dpo	1	0	1	0	0	1	0	1
18 dpo	1	0	0	1	0	1	0	1
23 dpo	1	0	1	1	0	1	0	1
28 dpo	1	0	1	1	0	1	1	1
30 dpo	1	0	1	1	0	1	1	1
35 dpo	0	1	1	1	1	1	1	1
49 dpo	0	1	1	1	1	1	1	1
55 dpo	0	1	1	1	1	1	1	1
62 dpo	0	1	1	1	1	1	1	1
68 dpo	0	1	1	1	1	1	1	1

TABLE 10. HNK-1 expression in different areas of *Pantherophis guttatus* embryonic hearts sampled at different developmental stages

AGE	AV-cushions	AV-canal	Sinus venosus	AV-sulcus—nerves	Ventricle	Atria	Valves	Aortic trunk
9 dpo	0	0	0	0	0	0	0	0
16 dpo	0	0	0	1	0	0	0	1
23 dpo	0	1	1	1	1	1	0	1
32 dpo	0	1	1	1	1	1	0	1

TABLE 11. HNK-1 expression in different areas of *Eublepharis macularius* embryonic hearts sampled at different developmental stages

AGE	AV-cushions	AV-canal	Sinus venosus	AV-sulcus—nerves	Ventriculus	Atria	Valves	Aortic trunk
7 dpo	0	0	0	0	0	0	0	0
11 dpo	0	0	0	0	0	0	0	1
15 dpo	1	0	0	1	0	0	0	1
18 dpo	0	0	1	1	0	1	1	1
26 dpo	0	0	1	1	0	1	1	1
32 dpo	0	0	1	1	1	1	1	1
40 dpo	0	1	1	1	1	1	1	1
47 dpo	0	0	1	1	1	1	1	1
53 dpo	0	0	0	1	0	1	1	0

TABLE 12. HNK-1 expression in different areas of *Gallus gallus* embryonic hearts sampled at different developmental stages

Incubation day	AV-cushions	AV-canal	Sinus venosus	AV-sulcus—nerves	Ventricle	Atria	Valves	Epicardium	His bundle
ED 4	1	1	1	0	1	1	0	1	0
ED 5	1	1	1	0	1	1	0	1	0
ED 6	1	1	1	1	1	1	0	1	0
ED 7	1	1	1	1	1	1	0	1	0
ED 8	1	1	1	1	1	1	1	1	1
ED 9	0	1	1	1	1	1	1	1	1
ED 10	0	1	1	1	1	1	1	1	1
ED 12	0	1	1	1	1	1	1	1	1
ED 13	0	1	1	1	1	1	1	1	1
ED 14	0	1	1	1	1	1	1	1	1
ED 16	0	1	1	1	1	1	1	1	1
ED 18	0	1	1	1	1	1	1	1	1
ED 20	0	1	1	1	1	1	1	1	1

Cardiac cushions are replaced by the valves at the fetal stages (after ED8).

Tween 20, 1% bovine serum albumin (BSA), and 10% NGS. The staining was performed in dark humid chamber. HRP activity was visualized using the diaminiobenzidine (DAB) as substrate.

After washing in distilled water, the nuclei were counterstained with hematoxylin. In the end, the sections were washed with distilled water and dehydrated in ascending series of ethanol (70%–100%), cleared in xylene, and mounted in Depex permanent medium (Electron Microscopy Sciences).

Sections were imaged on an Olympus virtual microscope (slide scanner, 10× objective, resolution 0.67 μm/pixel),

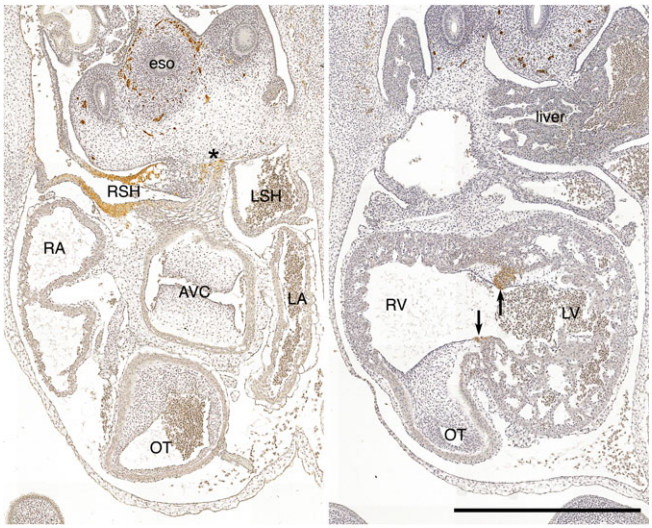

Fig. 1. Transverse sections through the heart of *Crocodylus niloticus*, 24 dpo. HNK-1 staining is apparent in the area of sinus venosus, in particular on the right side (left panel), nervous plexus around the esophagus (eso), and in a ring of ventricular myocytes surrounding the interventricular foramen (arrows, right panel). Asterisk indicates immunopositivity on the left side of the sinus venosus. AVC, atrioventricular canal, LA, left atrium, LSH, left sinus horn, LV, left ventricle, OT, outflow tract, RA, right atrium, RSH, right sinus horn, RV, right ventricle. Scale bar 1 mm.

and Olympus BX51 upright microscope using 2× and 4× objectives.

1.3 Double Immunofluorescence Staining

The sections were deparaffinized and rinsed once with PBS for 5 min, permeabilized twice with PBS/0.5% Tween 20 for 5 min, and rinsed once with PBS for 5 min. The slides for mouse monoclonal to Myosin Heavy Chain (MF20) antibody staining were heat-treated twice for 5 min in citrate buffer (pH 6.0) for antigen retrieval before blocking. Afterwards, the slides were cooled in PBS/0.5% Tween 20 for 10 min and then rinsed once with PBS for 5 min. All sections were blocked with 10% NGS for an hour at room temperature, and then incubated overnight at +4°C with mouse monoclonal HNK-1 primary antibody (1:50; Becton Dickinson #347390).

On the next day, the sections were rinsed in three changes of PBS and cyanine 5 (Cy5)-conjugated Goat Anti-Mouse secondary antibody (1:200; Jackson ImmunoResearch #115-175-075) was applied for 90 min at room temperature. After rinsing in PBS the sections were again blocked with 10% NGS for 1 h at room temperature, and incubated overnight at +4°C with the second primary mouse monoclonal antibody. The following antibodies and dilutions were used: mouse monoclonal to SMA (1:800; Sigma #A2547) or mouse monoclonal IgG2b isotype to myosine heavy chain (MF20, 1:5; DSHB #2147781).

On the third day, the sections were rinsed in three changes of PBS and then incubated with Alexa Fluor 488-conjugated Goat Anti-Mouse secondary antibody (1:200; Invitrogen # A11001), which was applied for 90 min at room temperature. Primary and secondary antibodies were diluted in PBS that contained 0.1% Tween 20, 1% BSA, and 10% NGS. The staining was performed in dark humid chamber.

After washing in distilled water, the nuclei were counterstained with Hoechst (1:100,000, Sigma #33342). In the end, the sections were washed with distilled water and dehydrated in ascending series of ethanol (70%–100%), cleared in xylene and mounted in Depex permanent medium (Electron Microscopy Sciences).

Sections were imaged on an Olympus FluoView laser-scanning confocal microscope using 4× and 10× objectives.

2. RESULTS

2.1 Nile Crocodile (*Crocodylus niloticus*, Laurenti 1768)

HNK-1 positive loci were observed consistently in peripheral nerves around the esophagus; the nerves did not invade the heart prior to 5 dpo (Stage 5). Within the heart, the immunopositivity was fairly regularly observed in the myocardium of sinus venosus from 6 dpo (Stage 10–11; Table 7). From 14 dpo (Stage 10) to 17 dpo (Stage 12), there was an additional transitory staining in a ring of myocytes surrounding the interventricular foramen (Fig. 1). No staining was observed at the stages examined in the cardiac cushions, or any other nonmyocardial components of the heart.

2.2 Mangrove Monitor (*Varanus indicus*, Daudin 1802)

Cardiac nerves, abundant around sinus venosus and the atrioventricular canal, were strongly positive in all examined specimens (Fig. 2). HNK-1 staining was consistently observed in the myocardium of the sinus venosus (on both sides, but stronger on the right one) in all examined hearts. In addition, staining was present in the extracellular matrix and mesenchymal cells of both atrioventricular as well as outflow tract cushions and later on the valves. Staining was invariably stronger in the outflow tract cushions (Fig. 2, Table 8), and at later stages, immunopositive cells (most likely of neural crest origin) were present on the outside of the great arteries and in the aorticopulmonary septum.

2.3 Central Bearded Dragon (*Pogona vitticeps*, Ahl 1926)

Already at the earliest stages (14 dpo), HNK-1 staining was present in the sinus venosus and the venous valve, as well as in the atrioventricular (stronger) and outflow tract (weaker staining intensity) cushions (Fig. 3). No labeling was present anywhere within the ventricle. Soon afterwards (18 dpo), staining appeared in the atrioventricular sulcus in association with the cardiac nerves (Table 9). At 28 dpo, staining was present in the interatrial septum; the positivity in the remodeling atrioventricular valves remained strong. By 35 dpo, staining appeared in some cells on the surface of the outflow tract, but no staining was present in the ventricle. By 39 dpo, staining appeared in some trabeculae and by 55 dpo, complete pattern including the outflow tract, mesenchymal, neuronal as well as myocardial staining, was present (Fig. 4). The myocardial positivity included areas of the

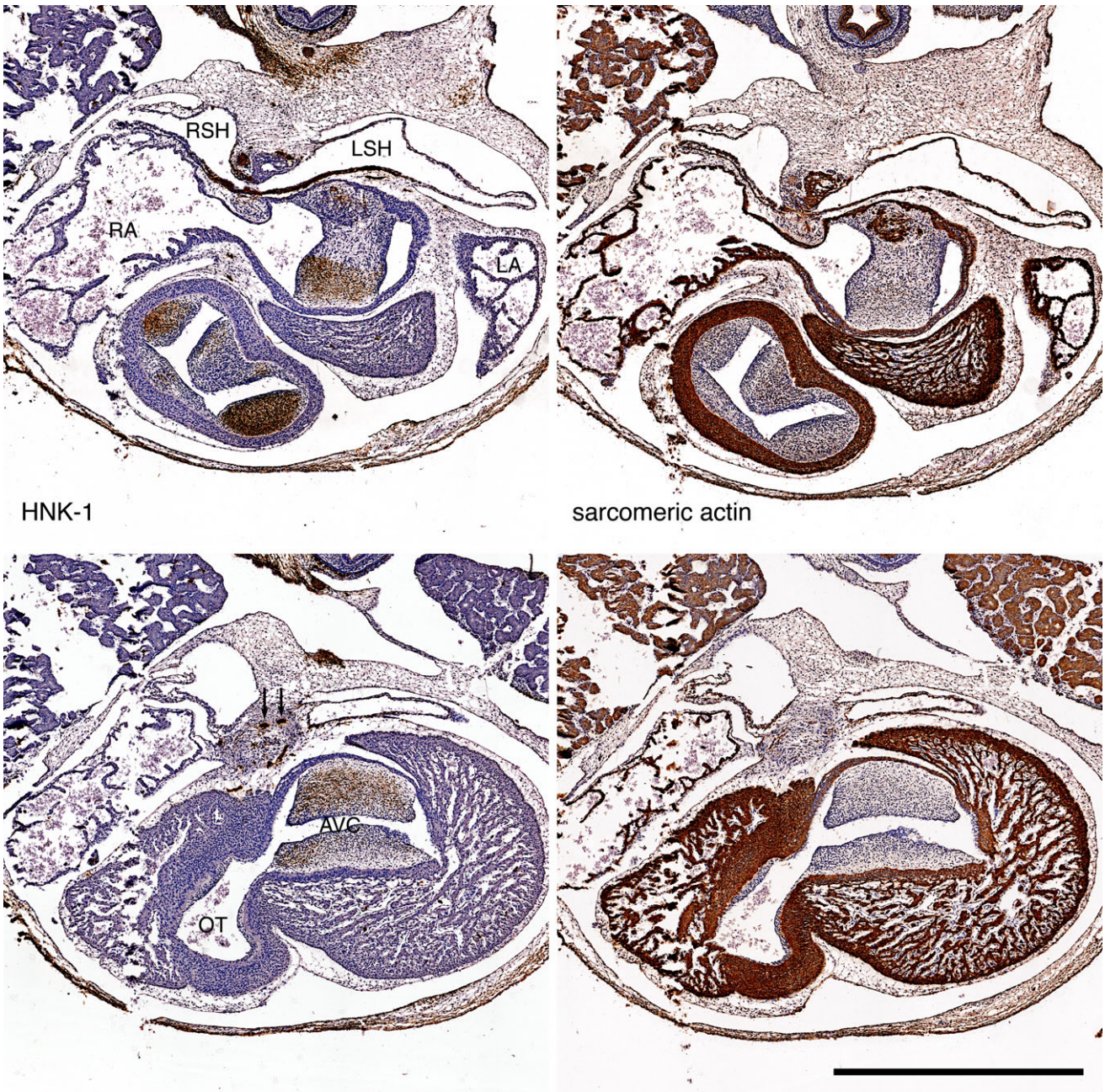

Fig. 2. Transverse sections through the heart of *Varanus indicus*, 43 dpo. HNK-1 staining is apparent in the areas of the atrioventricular and outflow cushions, as well as in other nearby mesenchymal tissues and nerves (arrows). Comparing with the myocardial marker staining on the right panels, the only myocytes labeled are those of the sinus venosus. AVC, atrioventricular canal, LA, left atrium, LSH, left sinus horn, OT, outflow tract, RA, right atrium, RSH, right sinus horn. Scale bar 0.1 mm.

sinus venosus, pectinate muscles in the atria, atrioventricular canal, and ventricular septum. This pattern persisted until the last stage examined (68 dpo).

2.4 Corn Snake (*Pantherophis guttatus*, Linnaeus 1766)

At an early stage of 9 dpo there was no positivity for HNK-1 in any heart compartments. At stage of 16 dpo the nerves in sulcus coronarius became positive for HNK-1. At stage of 23 dpo, however, the positivity was observed along the atrioventricular canal on both sides and in the bulbuslamelle of the ventricle very close to the right part of the atrioventricular canal as well as in the nerves in sulcus coronarius. Positivity was observed also in the interatrial septum. However, there was no observation of positivity in the ventricular valves as well as in the deep ventricle subendocardium (Fig. 5, Table 10). At stage of 32 dpo there was a similar staining pattern as at the previous stage and also a slight positivity in the area

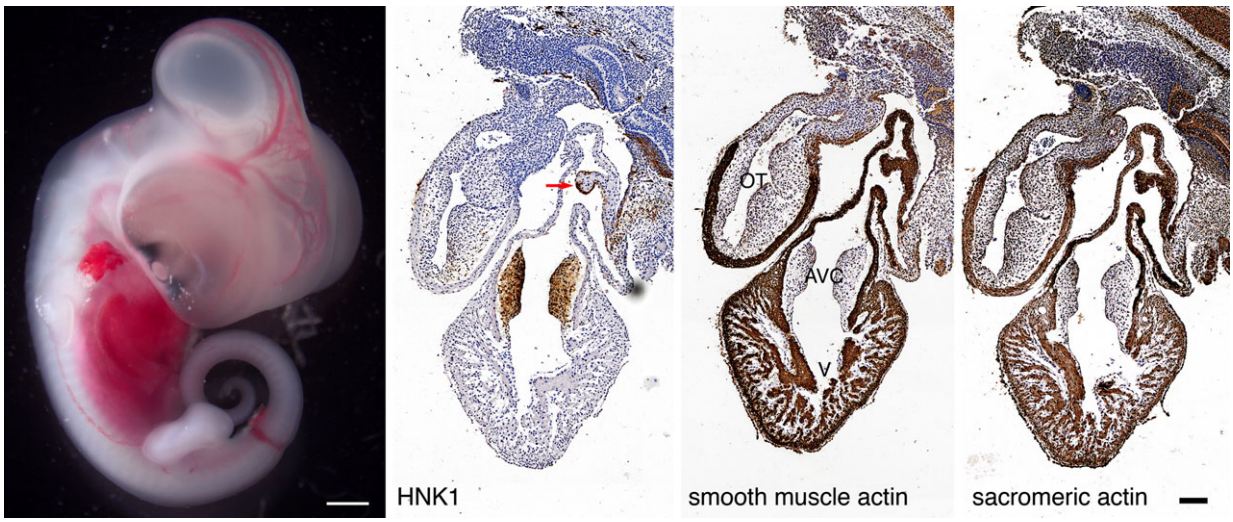

Fig. 3. Right profile of the whole embryo of *Pogona vitticeps* (14 dpo) and frontal sections through its heart. HNK-1 staining is apparent in the areas of the atrioventricular cushions and in the mesenchymal cap of the interatrial septum (arrow). Very faint staining is present at the base of the outflow cushions. Other mesenchymal and neural structures are also positive in the adjacent areas. Myocardial markers show that there are no myocytes positive at this stage. AVC, atrioventricular canal, OT, outflow tract, V, ventricle, scale bars 1 mm for the whole embryo, 0.1 mm for the sections.

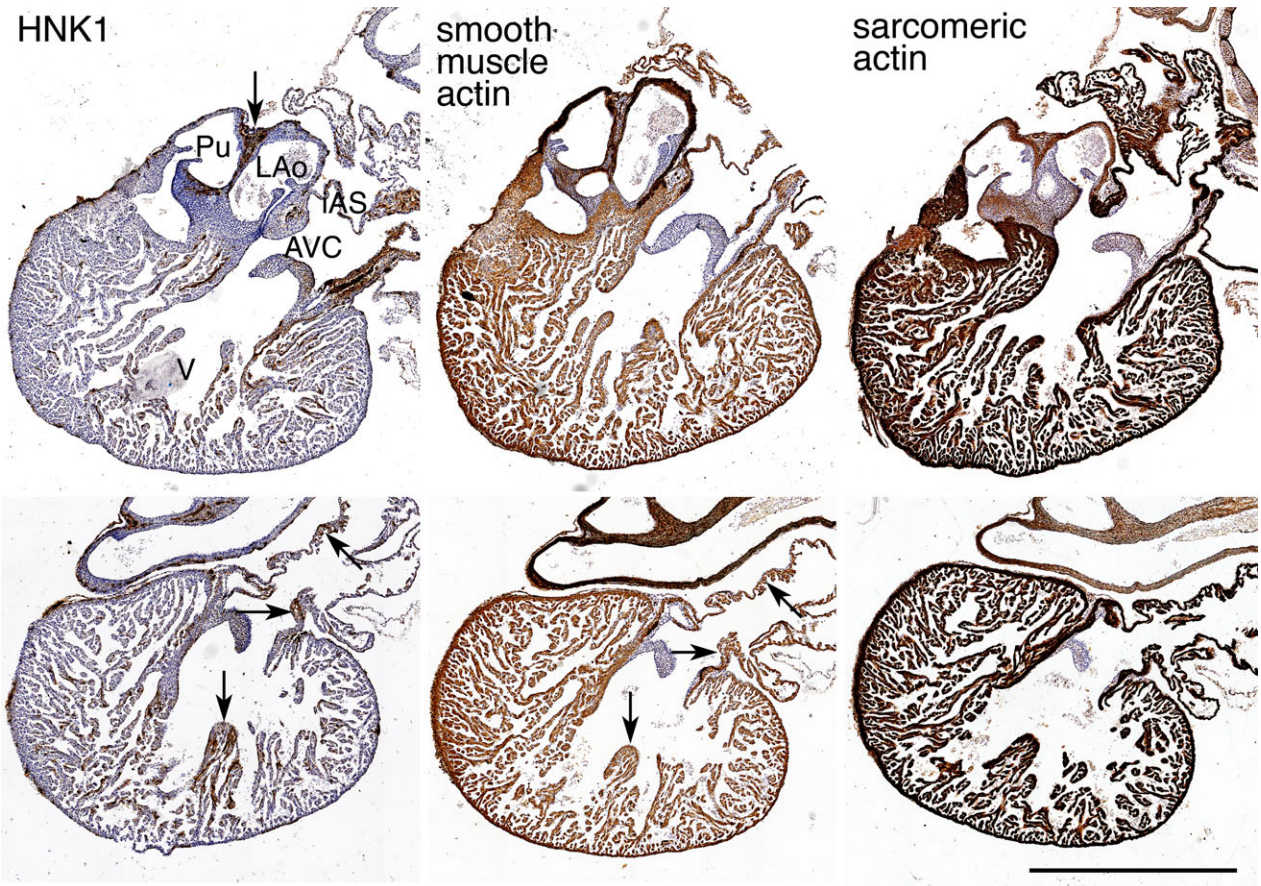

Fig. 4. Frontal sections through the heart of *Pogona vitticeps,* 55 dpo. HNK-1 staining is apparent in the areas of the atrioventricular and outflow cushions transforming into the valves and in the aorticopulmonary septum (IAS, arrow). Staining is also present in the epicardium and mesenchyme of the atrioventricular sulcus. Myocardial markers show that there is positivity in the myocytes of the interatrial septum, atrioventricular canal (AVC) as well as the ventricular septum (arrows in bottom panels) and some ventricular trabeculae at this stage. LAo, left aorta, Pu, pulmonary artery, scale bars 1 mm.

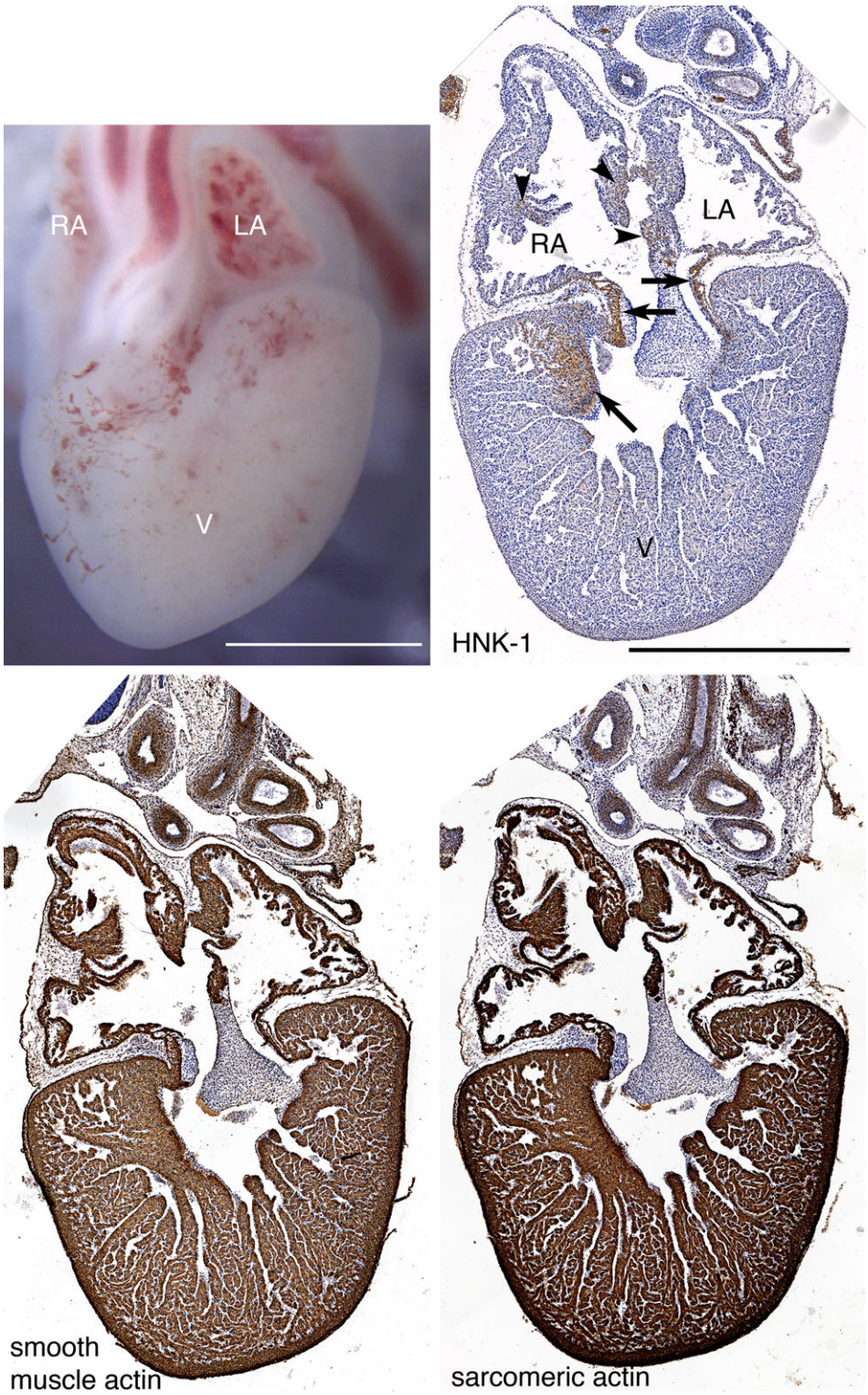

Fig. 5. Whole heart of *Pantherophis guttatus* (23 dpo) and frontal sections through it. HNK-1 staining is apparent in the area of the putative internodal tracts in the atria (arrowheads), the atrioventricular canal, and the bulbuslamelle in the ventricle (arrows). The wall of the left sinus horn (*) is also positive. While the nerves are also positive, no mesenchymal structures are stained. LA, left atrium, RA, right atrium, V, ventricle. Scale bar 1 mm.

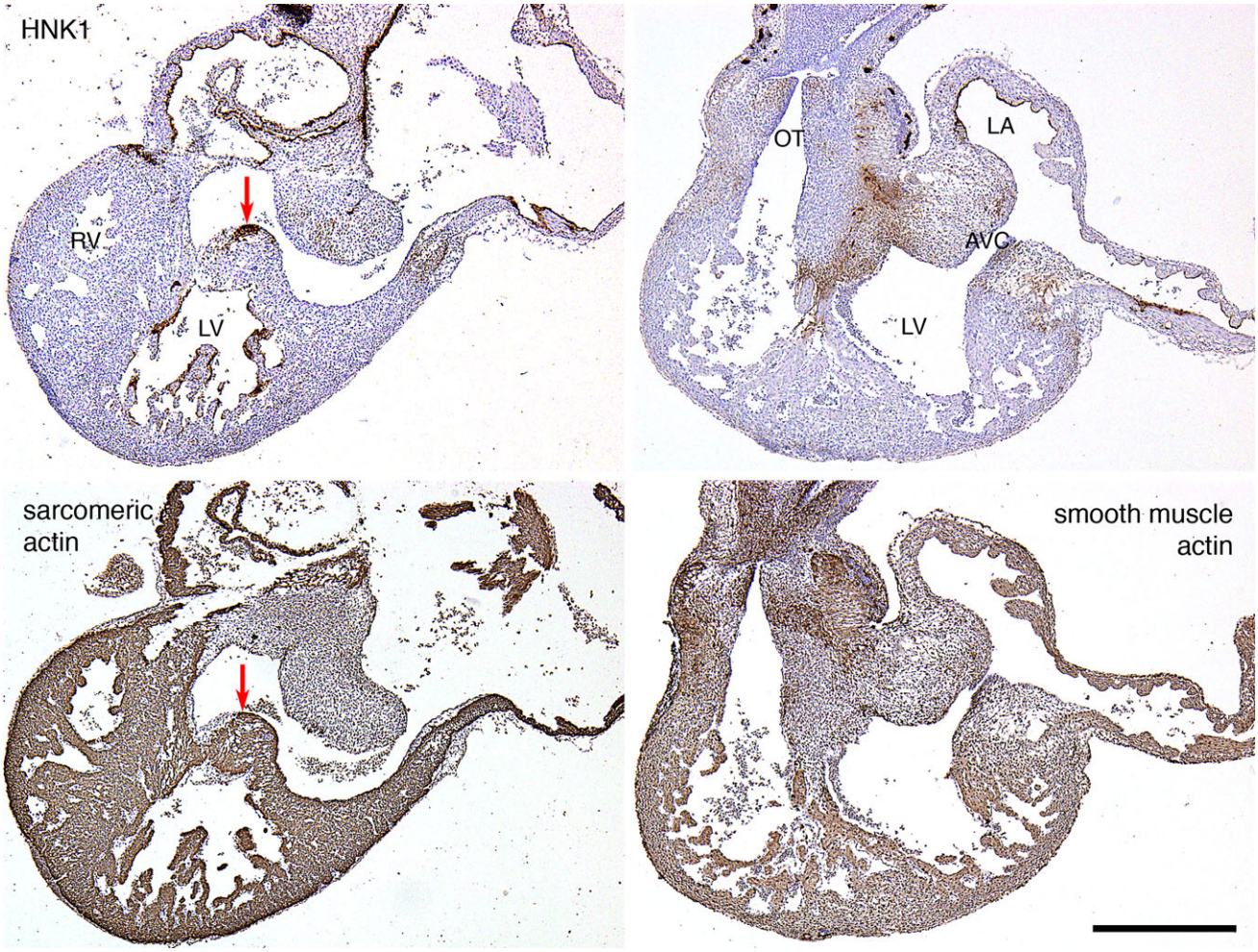

Fig. 6. Frontal sections through the heart of *Gallus gallus,* 7 dpo (embryonic day 7). HNK-1 staining is apparent in the areas of the atrial and left ventricular subendocardium, as well as in the cardiac mesenchymal tissues. Arrows point to the location of the myocardial atrioventricular (His) bundle. AVC, atrioventricular canal, LA, left atrium, LV, left ventricle, OT, outflow tract, RA, right atrium, RV, right ventricle. Scale bar 1 mm.

of forming ventricular septum, the bulbuslamelle, and the pectinate muscles. Taken together, the heart of *Pantherophis* showed relatively low positivity for HNK-1 in comparison to the previous lizard species examined, that is, *Varanus* and *Pogona.*

2.5 Leopard Gecko (*Eublepharis macularius*, Blyth 1854)

In the hearts examined, no cardiac staining was observed until 11 dpo (Table 11). From 15 dpo, immunopositive cells were observed on the surface of the outflow tract. By this stage, nerves appeared in the atrioventricular sulcus area. Weak staining was also detected in the atrioventricular and outflow tract cushions. By 18 dpo, strongly positive nerves were observed in the subepicardium across the entire ventricle. However, no staining was present within the ventricle, which, in contrast to previous two lizard species, did not show any conspicuous ventricular septum (data not shown). Myocardial staining was, however, seen the sinus venosus at most stages, but only at 40 dpo in the atrioventricular canal in this species (Table 11).

2.6 Domestic Fowl (*Gallus gallus f. domestica*, Linnaeus 1758)

In agreement with numerous previous observations including our own, we confirmed the presence of HNK-1 staining in the area of developing cardiac cushions, nerves, and neural crest cells. Staining was present in and around the His bundle but not in the bundle branches or more peripheral components. Strong and consistent staining was also present in the subendocardium of both the atria and ventricles (Figs. 6 and 7, Table 12). In comparison with the slides from our previous study (Gurjarpadhye et al., 2007) as well as with freshly sampled and stained hearts at the same stage, we did not observe any differences in the staining pattern between the paraformaldehyde- or Dent's (methanol/DMSO)-fixed tissue.

Double immunohistochemistry was used to confirm the specificity of myocardial in the avian heart. Chick heart at ED12 (Fig. 8) stained simultaneously for myosine heavy chain and HNK-1 showed clearly the myocardial character of HNK-1 positive cells within the interventricular septum (His bundle and surrounding area). To validate that such

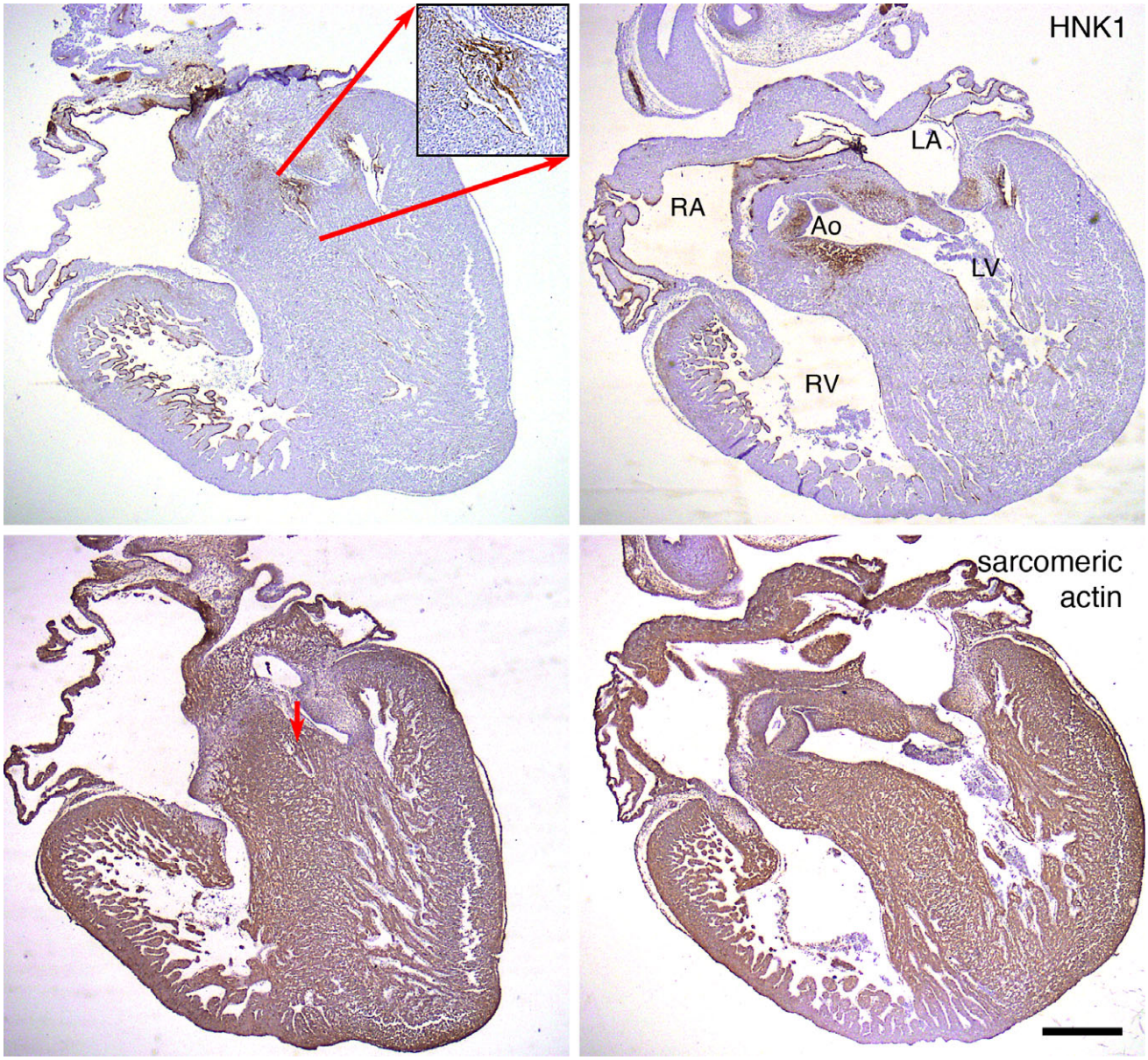

Fig. 7. Frontal sections through the heart of *Gallus gallus,* 10 dpo (embryonic day 10). HNK-1 staining is apparent in the areas of the atrial and ventricular subendocardium, and developing atrioventricular and semilunar valves. Arrows point to the location of the myocardial atrioventricular (His) bundle, which is positive as well as its fibrous insulation. Ao, aorta, LA, left atrium, LV, left ventricle, RA, right atrium, RV, right ventricle. Scale bar 1 mm.

pattern is not unique to this species, we also stained ED8 quail embryonic heart obtained in a context of a different study (Nanka et al., 2008). Indeed, the HNK-1 staining pattern was the same as in the chick, illustrated by double immunopositivity of the sinus venosus myocardium (Fig. 8).

3. DISCUSSION

Our findings in the reptilian hearts correspond well with the results in reported in other amniote species. We found expression in the developing cardiac cushions/valves, which is very similar to situation reported in the chick, attesting to phylogenetic proximity between reptiles and birds (Laurin and Reisz, 1995). Similarly, in all of our species we confirmed expression in the myocardium of the sinus venosus (Tables 7–12), making it a good maker of the pacemaker regions as in rat and human embryos (Blom et al., 1999). Most interesting was the finding of positivity in the ventricular myocardium, specifically a ring-like structure reminiscent of the primary interventricular ring, in the *Crocodylus* and in the trabeculae forming, or close to, the ventricular septum in *Pogona*. These findings suggest that the phylogenetic origin of the ventricular conduction system may lie in the reptilian lineage; however, functional studies are needed

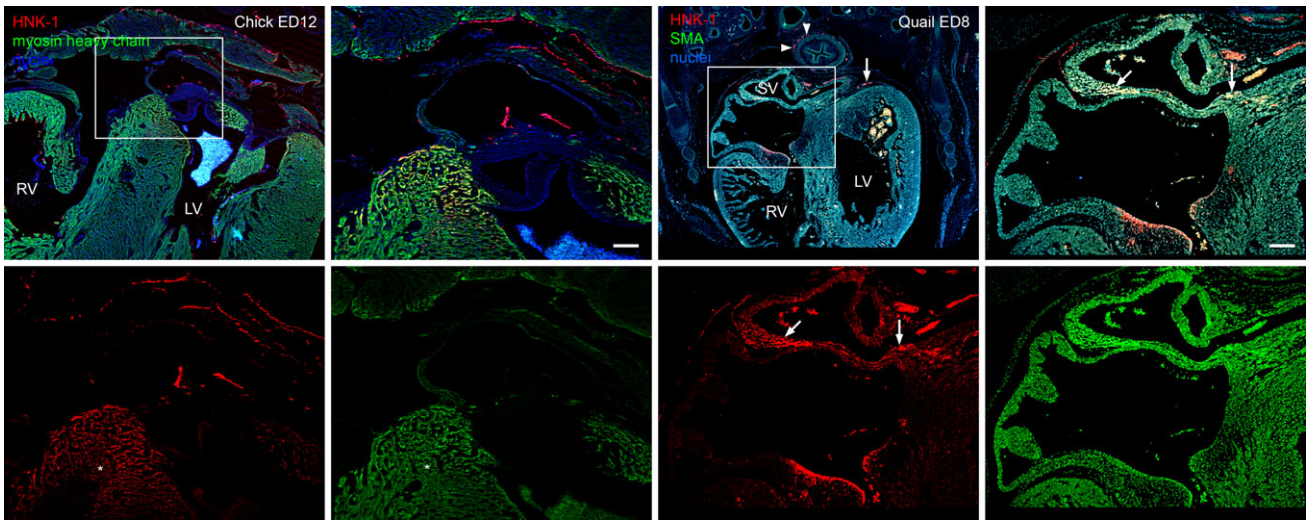

Fig. 8. Double immunohistochemistry for HNK-1 (red channel) and myocyte markers (green) in avian heart. In mid-fetal chick, co-localization is observed in the area of the interventricular septum, where the His bundle (asterisk in the higher power views) is present. In early postseptaion quail heart, double positivity is present in the myocardium of the sinus venosus (arrows in the higher power view); the staining is more prominent on the right side. Non-myocardial staining in the right atrioventricular valve is also prominent. Single positivity for HNK-1 is present also in the nervous plexus around the esophagus (arrowheads in the overview picture) as well as cardiac nerves in the atrioventricular sulcus (arrow). Scale bar 100 μm; nuclear staining (Hoechst) is in the blue channel. LV, left ventricle, RV, right ventricle, SV, sinus venosus.

to confirm these observations, as the presence of ventricular conduction system is normally considered to be a feature associated with homeiothermy (Davies and Francis, 1941) and thus limited to birds and mammals.

Expression of the HNK-1 carbohydrate epitope in developing hearts of the reptilian embryos occurs in morphologically dynamic regions such the developing atrioventricular valves, outflow tract cushions, autonomic nervous system of the heart, and differentiating CCS. The antibody was first described in 1981 (Abo and Balch, 1981), and to date (May 31, 2018), there are 2,493 hits on PubMed, contesting to the potential of this IgM monoclonal antibody. Expression in the developing heart was first reported in association with its innervation in the rabbit (Gorza et al., 1988), and already there it was associated with the CCS as well as neural crest cells. Most detailed mammalian studies were soon afterwards performed in the rat (Ikeda et al., 1990), which appears to have the same pattern of expression as the developing human heart (Blom et al., 1999). The pattern consists of two rings, the atrioventricular one (corresponding to the atrioventricular canal myocardium) and the interventricular one (also known as the primary interventricular ring), which forms a preferential pathway in early ventricular activation (Sedmera et al., 2005; Sankova et al., 2012). This expression was later confirmed by three-dimensional reconstructions (Ito et al., 1992; Nakagawa et al., 1993; Wenink et al., 2000) and added to the map was an additional domain in the atria—the sinus venosus-derived pacemaker tissue and the intermodal tracts. We observed similar positivity in the pectinate muscles, especially in the right atrium, in *Pogona* and *Pantherophis* (Figs. 4 and 5).

Studies in the avian embryos followed shortly, and in chick and quail hearts, good correlation was found between the HNK-1 expression and forming His bundle and proximal parts of its branches (Luider et al., 1993; Chuck and Watanabe, 1997; Wikenheiser et al., 2006) as well as the pacemaker region in the atria (DeRuiter et al., 1995). Most of these studies used also additional markers to confirm specificity of expression, thus validating this antibody as a (temporal) marker of the CCS. Indeed, *in vitro* study on cultured precardiac mesoderm cells (Nakajima et al., 2001) showed that there are at least three cell types, that is, mesenchymal cells with HNK-1 positivity, and positive and negative cardiomyocytes. However, the HNK-1 is not, unlike, for example, some ion channels or gap junction proteins, a functional marker—and indeed is absent from the conduction system in the mouse. Thus, functional studies using electrophysiological approaches will be needed to validate further our immunohistochemical findings. Alternatively, specificity could be confirmed using double immunohistochemistry for other proteins expressed in the CCS. Such alternative/additional immunohistochemical markers, which again can be species-specific, include neurofilament 1 in the rabbit (Gorza et al., 1988; Rothenberg et al., 2005), PGP9.5 in the camel (El Sharaby et al., 2001), or Contractin-2 in the mouse (Pallante et al., 2010).

Although some ECG recordings were performed in Sauropsida in general (Kaplan and Schwartz, 1963; McDonald and Heath, 1971; Blanco, 1993; Heaton-Jones and King, 1994; Anderson et al., 1999; Espino et al., 2001; Martinez-Silvestre et al., 2003; Tan et al., 2013), the information available is restricted to a few species and there are almost no comparative studies among Squamate reptiles (Mullen, 1967; Bogan Jr., 2017) to fully understand the electrophysiological function of the heart in these terrestrial ectotherms. However, with respect to ECG methodology (Einthoven, 1903), there are also some limitations of this approach for poikilotherms and ectotherms. Effect of the temperature on cardiac function is relatively profound (Vostarek et al., 2016), especially in ectotherms such as squamates (C-B and R-D, 2005), and also the impact of the anesthesia could be noticeable (Anderson et al., 1999; Kharin and Shmakov, 2009).

Therefore, it is useful to complement the electrophysiological methods with histology providing structure—function correlation in the hearts of sauropsid species (this study).

In conclusion, HNK-1 immunoreactivity in the developing sauropsid heart includes parts of the early outflow tract, most likely of neural crest origin (Kirby and Waldo, 1990), the related endocardial cushions, the primordia of the semilunar valve leaflets and the aorticopulmonary septum. Furthermore, other mesenchymal structures are HNK-1 positive, such as the atrioventricular cushions, spina vestibuli, and parts of the subendocardium. Last, staining includes regions of the myocardium that are part of the forming CCS, specifically, the wall of the sinus venosus, interatrial septum, internodal pathways, atrioventricular canal, and possibly also the nascent ventricular conduction system. We believe that the differences in expression observed are mostly due to species-specificity (as in mammals) and the extent of ventricular septation.

3.1 Study Limitations

The function of the HNK-1 glycoprotein antigen is not completely understood in part because there is no clean way to delete the antigen. In general, there is a correlation and association of the antigen with migratory, plastic, or dynamic interactions. Functional studies including electrophysiology (Gregorovicova et al., 2018) might help in correlating the present findings with activation patterns of squamate reptilian hearts at different developmental stages.

ACKNOWLEDGMENTS

We thank the reptile breeders Martina Gregorovičová, Martin Kotal, and Petr Velenský for providing the eggs of *Pogona*, *Eublepharis, Pantherophi*s, and *Varanus*, and Ms. Jarmila Svatůšková, Klára Krausová, Blanka Topinková, and Marie Jindráková for their excellent technical assistance. This study was supported by grant 16-02972S and 13-12412S from the Grant Agency of the Czech Republic, Ministry of Education, Youth and Sports of the Czech Republic PROGRES-Q38 and COST LTC17023, MEYS (LM2015062 Czech-BioImaging), and Czech Academy of Sciences RVO: 67985823. M.K. thanks Samuel Martin for his permission to collect the *C. niloticus* embryos at La Ferme aux Crocodiles (LFAC, Pierrelatte, France), as well as S. Martin and Vincent Lancelle (LFAC) for their risky assistance in removing eggs from the nesting area. This article has been prepared for a special issue of *Anatomical Record* in honor of Roger R. Markwald.

LITERATURE CITED

Abo T, Balch CM. 1981. A differentiation antigen of human NK and K cells identified by a monoclonal antibody (HNK-1). J Immunol 127:1024–1029.

Adolph SC, Porter WP. 1993. Temperature, activity, and lizard life histories. Am Nat 142:273–295.

Anderson NL, Wack RF, Calloway L, Hetherington TE, Williams JB. 1999. Cardiopulmonary effects and efficacy of propofol as an anesthetic agent in brown tree snakes, *Boiga irregularis*. Bull Assoc Rept Amphib Vet 9:9–17.

Aoyama N, Kikawada R, Yamashina S. 1993. Immunohistochemical study on the development of the rat heart conduction system using anti-Leu-7 antibody. Arch Histol Cytol 56:303–315.

Benton MJ, Clark JM. 1988. Archosaur phylogeny and the relationships of the crocodylia. In: Benton MJ, editor. *The phylogeny and classification of the tetrapods*, Vol. 1. Oxford: Clarendon Press. p 295–338.

Blanco J. 1993. Avian electrocardiography: a contribution for the practitioner. In: Proceedings of the 1993 European conference on avian medicine and surgery. Association of *Avian* Veterinarians, Utrecht, p 137-154.

Blom NA, Gittenberger-de Groot AC, DeRuiter MC, Poelmann RE, Mentink MM, Ottenkamp J. 1999. Development of the cardiac conduction tissue in human embryos using HNK-1 antigen expression: possible relevance for understanding of abnormal atrial automaticity. Circulation 99:800–806.

Bogan JE Jr. 2017. Ophidian cardiology—a review. J Herpetolog Med Surg 27:62–77.

Burggren W. 1988. Cardiac design in lower vertebrates: what can phylogeny reveal about ontogeny? Experientia 44:919–930.

Chiari Y, Cahais V, Galtier N, Delsuc F. 2012. Phylogenomic analyses support the position of turtles as the sister group of birds and crocodiles (Archosauria). BMC Biol 10:65.

Chuck ET, Watanabe M. 1997. Differential expression of PSA-NCAM and HNK-1 epitopes in the developing cardiac conduction system of the chick. Dev Dyn 209:182–195.

Cree A. 2014. *Tuatara: biology and conservation of a venerable survivor*. Christchurch, New Zealand: Canterbury University Press.

Davies F. 1942. The conducting system of the vertebrate heart. Br Heart J 4:66–76.

Davies F, Francis ETB. 1941. The heart of the salamander (*Salamandra salamandra* L.), with special refernce to the conducting (connecting) system and its bearing on the phylogeny of the conducting systems of mammalian and avian hearts. Phil Trans R Soc B 231:99–139.

DeRuiter MC, Gittenberger-De Groot AC, Wenink AC, Poelmann RE, Mentink MM. 1995. In normal development pulmonary veins are connected to the sinus venosus segment in the left atrium. Anat Rec 243:84–92.

Einthoven W. 1903. Die galvanometrische Registrirung des menschlichen Elektrokardiogramms, zugleich eine Beurtheilung der Anwendung des Capillar-Elektrometers in der Physiologie. Archiv für die gesamte Physiologie des Menschen und der Tiere 99:472–480.

El Sharaby AA, Egerbacher M, Hammoda AK, Bock P. 2001. Immunohistochemical demonstration of Leu-7 (HNK-1), neurone-specific enolase (NSE) and protein-gene peptide (PGP) 9.5 in the developing camel (*Camelus dromedarius*) heart. Anat Histol Embryol 30:321–325.

Espino L, Suárez ML, López-Beceiro A, Santamarina G. 2001. Electrocardiogram reference values for the buzzard in Spain. J Wildl Dis 37:680–685.

Gorza L, Schiaffino S, Vitadello M. 1988. Heart conduction system: a neural crest derivative? Brain Res 457:360–366.

Gregorovicova M, Sedmera D, Jensen B. 2018. Relative position of the atrioventricular canal determines the electrical activation of developing reptile ventricles. J Exp Biol 221:jeb178400.

Gregorovicova M, Zahradnicek O, Tucker AS, Velensky P, Horacek I. 2012. Embryonic development of the monitor lizard, *Varanus indicus*. Amphib Rept 33:451–468.

Grigg GC, Kirshner D. 2015. *Biology and evolution of Crocodylians*. Clayton, Victoria: CSIRO Publishing.

Gurjarpadhye A, Hewett KW, Justus C, Wen X, Stadt H, Kirby ML, Sedmera D, Gourdie RG. 2007. Cardiac neural crest ablation inhibits compaction and electrical function of conduction system bundles. Am J Physiol Heart Circ Physiol 292: H1291–H1300.

Heaton-Jones TG, King RR. 1994. Characterization of the electrocardiogram of the American alligator (*Alligator mississippiensis*). J Zoo Wildl Med 25:40–47.

Hicks JW, Wang T. 1996. Functional role of cardiac shunts in reptiles. J Exp Zool A Ecol Genet Physiol 275:204–216.

Ikeda T, Iwasaki K, Shimokawa I, Sakai H, Ito H, Matsuo T. 1990. Leu-7 immunoreactivity in human and rat embryonic hearts, with special reference to the development of the conduction tissue. Anat Embryol (Berl) 182:553–562.

Ito H, Iwasaki K, Ikeda T, Sakai H, Shimokawa I, Matsuo T. 1992. HNK-1 expression pattern in normal and bis-diamine induced

malformed developing rat heart: three dimensional reconstruction analysis using computer graphics. Anat Embryol (Berl) 186:327–334.
Jensen B, Boukens BJ, Postma AV, Gunst QD, van den Hoff MJ, Moorman AF, Wang T, Christoffels VM. 2012. Identifying the evolutionary building blocks of the cardiac conduction system. PLoS One 7:e44231.
Jensen B, Moorman AF, Wang T. 2014. Structure and function of the hearts of lizards and snakes. Biol Rev Camb Philos Soc 89:302–336.
Jensen B, Nyengaard JR, Pedersen M, Wang T. 2010. Anatomy of the python heart. Anat Sci Int 85:194–203.
Jensen B, van den Berg G, van den Doel R, Oostra RJ, Wang T, Moorman AF. 2013a. Development of the hearts of lizards and snakes and perspectives to cardiac evolution. PLoS One 8:e63651.
Jensen B, Wang T, Christoffels VM, Moorman AF. 2013b. Evolution and development of the building plan of the vertebrate heart. Biochim Biophys Acta 1833:783–794.
Kaplan HM, Schwartz C. 1963. Electrocardiography in turtles. Life Sci 2:637–645.
Kharin S, Shmakov D. 2009. A comparative study of contractility of the heart ventricle in some ectothermic vertebrates. Acta Herpetolog 4:57–71.
Kirby ML, Waldo KL. 1990. Role of neural crest in congenital heart disease. Circulation 82:332–340.
Köhler G, Griesshammer K, Schuster N. 2003. *Bartagamen Lebensweise, Haltung, Zucht, Erkrankungen*. Germany: Herpeton.
Koshiba-Takeuchi K, Mori AD, Kaynak BL, Cebra-Thomas J, Sukonnik T, Georges RO, Latham S, Beck L, Henkelman RM, Black BL. 2009. Reptilian heart development and the molecular basis of cardiac chamber evolution. Nature 461:95–98.
Kundrat M. 2008. HNK-1 immunoreactivity during early morphogenesis of the head region in a nonmodel vertebrate, crocodile embryo. Naturwissenschaften 95:1063–1072.
Kundrat M. 2009. Heterochronic shift between early organogenesis and migration of cephalic neural crest cells in two divergent evolutionary phenotypes of archosaurs: crocodile and ostrich. Evol Dev 11:535–546.
Laurin M, Reisz RR. 1995. A reevaluation of early amniote phylogeny. Zool J Linn Soc-Lond 113:165–223.
Lee MSY. 1997. The phylogeny of varanoid lizards and the affinities of snakes. Philos T R Soc B 352:53–91.
C-B L, R-D L. 2005. Electrocardiogram and heart rate in response to temperature acclimation in three representative vertebrates. Comp Biochem Physiol A Mol Integr Physiol 142:416–421.
Luider TM, Bravenboer N, Meijers C, van der Kamp AW, Tibboel D, Poelmann RE. 1993. The distribution and characterization of HNK-1 antigens in the developing avian heart. Anat Embryol (Berl) 188:307–316.
Martinez-Silvestre A, Mateo J, Pether J. 2003. Electrocardiographic parameters in the Gomeran giant lizard, *Gallotia bravoana*. J Herpetolog Med Surg 13:22–25.
McDonald HS, Heath JE. 1971. Electrocardiographic observations on the tuatara, *Sphenodon punctatus*. Comp Biochem Physiol A Physiol 40:881–892.
Moorman AF, Christoffels VM. 2003. Cardiac chamber formation: development, genes, and evolution. Physiol Rev 83:1223–1267.
Mullen RK. 1967. Comparative electrocardiography of squamata. Physiol Zool 40:114–126.
Nakagawa M, Thompson RP, Terracio L, Borg TK. 1993. Developmental anatomy of HNK-1 immunoreactivity in the embryonic rat heart: co-distribution with early conduction tissue. Anat Embryol (Berl) 187:445–460.
Nakajima Y, Yoshimura K, Nomura M, Nakamura H. 2001. Expression of HNK1 epitope by the cardiomyocytes of the early embryonic chick: in situ and in vitro studies. Anat Rec 263:326–333.
Nanka O, Krizova P, Fikrle M, Tuma M, Blaha M, Grim M, Sedmera D. 2008. Abnormal myocardial and coronary vasculature development in experimental hypoxia. Anat Rec (Hoboken) 291:1187–1199.
Nesbitt SJ, Desojo JB, Irmis RB. 2013. Anatomy, phylogeny and palaeobiology of early archosaurs and their kin. Geol Soc Lond Spec Publ 379:1–7.
Nordlander RH. 1989. HNK-1 marks earliest axonal outgrowth in Xenopus. Brain Res Dev Brain Res 50:147–153.
Pallante BA, Giovannone S, Fang-Yu L, Zhang J, Liu N, Kang G, Dun W, Boyden PA, Fishman GI. 2010. Contactin-2 expression in the cardiac Purkinje fiber network. Circ Arrhythm Electrophysiol 3:186–194.
Pianka E, King D. 2004. *Varanoid lizards of the world*. Indiana, IN: Indiana University Press.
Poelmann RE, Gittenberger-de Groot AC, Biermans MW, Dolfing AI, Jagessar A, Hattum S, Hoogenboom A, Wisse LJ, Vicente-Steijn R, Bakker MA. 2017. Outflow tract septation and the aortic arch system in reptiles: lessons for understanding the mammalian heart. EvoDevo 8:9.
Pyron RA, Burbrink FT, Wiens JJ. 2013. A phylogeny and revised classification of Squamata, including 4161 species of lizards and snakes. BMC Evol Biol 13:93.
Rest JS, Ast JC, Austin CC, Waddell PJ, Tibbetts EA, Hay JM, Mindell DP. 2003. Molecular systematics of primary reptilian lineages and the tuatara mitochondrial genome. Mol Phylogenet Evol 29:289–297.
Rothenberg F, Nikolski V, Watanabe M, Efimov I. 2005. Electrophysiology and anatomy of embryonic rabbit hearts before and after septation. Am J Physiol Heart Circ Physiol 288:H344–H351.
Sankova B, Benes J Jr, Krejci E, Dupays L, Theveniau-Ruissy M, Miquerol L, Sedmera D. 2012. The effect of connexin40 deficiency on ventricular conduction system function during development. Cardiovasc Res 95:469–479.
Sedmera D, Reckova M, Rosengarten C, Torres MI, Gourdie RG, Thompson RP. 2005. Optical mapping of electrical activation in developing heart. Microscop Microanal 11:209–215.
Seufer H, Kaverkin Y, Kirschner A. 2005. *The eyelash geckos: care, breeding and natural history*. Rheinstetten, Germany: Kirschner & Seufer Verlag.
Shine R. 2005. Life-history evolution in reptiles. Annu Rev Ecol Evol Syst 36:23–46.
Tan YFS, Gicana KRB, Lastica EA. 2013. Electrocardiographis profile of captive marbled water monitor lizard (*Varanus marmoratus*, Weigmann, 1834). Philipp J Vet Anim Sci 39:269–876.
Thompson GG, Withers PC. 1997. Standard and maximal metabolic rates of goannas (Squamata: Varanidae). Physiol Zool 70:307–323.
Vidal N, Hedges SB. 2005. The phylogeny of squamate reptiles (lizards, snakes, and amphisbaenians) inferred from nine nuclear protein-coding genes. C R Biol 328:1000–1008.
Vostarek F, Svatunkova J, Sedmera D. 2016. Acute temperature effects on function of the chick embryonic heart. Acta Physiolog 217:276–286.
Wang T, Altimiras J, Klein W, Axelsson M. 2003. Ventricular haemodynamics in *Python molurus*: separation of pulmonary and systemic pressures. J Exp Biol 206:4241–4245.
Webb G, Heatwole H, De Bavay J. 1971. Comparative cardiac anatomy of the reptilia. I. The chambers and septa of the varanid ventricle. J Morphol 134:335–350.
Webb GJ. 1979. Comparative cardiac anatomy of the reptilia. III. The heart of crocodilians and an hypothesis on the completion of the interventricular septum of crocodilians and birds. J Morphol 161:221–240.
Webb GJ, Heatwole H, de Bavay J. 1974. Comparative cardiac anatomy of the reptilia. II. A critique of the literature on the squamata and rhynchocephalia. J Morphol 142:1–20.
Wenink AC, Symersky P, Ikeda T, DeRuiter MC, Poelmann RE, Gittenberger-de Groot AC. 2000. HNK-1 expression patterns in the embryonic rat heart distinguish between sinuatrial tissues and atrial myocardium. Anat Embryol (Berl) 201:39–50.
White FN. 1968. Functional anatomy of the heart of reptiles. Am Zool 8:211–219.
Wiens JJ, Slingluff JL. 2001. How lizards turn into snakes: a phylogenetic analysis of body-form evolution in anguid lizards. Evolution 55:2303–2318.
Wikenheiser J, Doughman YQ, Fisher SA, Watanabe M. 2006. Differential levels of tissue hypoxia in the developing chicken heart. Dev Dyn 235:115–123.
Wilson SW, Ross LS, Parrett T, Easter SS Jr. 1990. The development of a simple scaffold of axon tracts in the brain of the embryonic zebrafish, Brachydanio rerio. Development 108:121–145.